

## NON-PERIODIC GEODESIC BALL PACKINGS GENERATED BY INFINITE REGULAR PRISM TILINGS IN $\widetilde{\mathbf{SL}_2\mathbf{R}}$ SPACE

JENŐ SZIRMAI

ABSTRACT. In [14] we defined and described the *regular infinite or bounded*  $p$ -gonal prism tilings in  $\widetilde{\mathbf{SL}_2\mathbf{R}}$  space. We proved that there exist infinitely many regular infinite  $p$ -gonal face-to-face prism tilings  $\mathcal{T}_p^i(q)$  and infinitely many regular bounded  $p$ -gonal non-face-to-face prism tilings  $\mathcal{T}_p(q)$  for integer parameters  $p, q$ ,  $3 \leq p$ ,  $2p/(p-2) < q$ . Moreover, in [5, 7] we have determined the symmetry group of  $\mathcal{T}_p(q)$  via its index 2 rotational subgroup, denoted by  $\mathbf{pq2}_1$  and investigated the corresponding geodesic and translation ball packings.

In this paper, we study the structure of the regular infinite or bounded  $p$ -gonal prism tilings and we prove that the side curves of their base figures are arcs of Euclidean circles for each parameter. Furthermore, we examine the non-periodic geodesic ball packings of congruent regular non-periodic prism tilings derived from the regular infinite  $p$ -gonal face-to-face prism tilings  $\mathcal{T}_p^i(q)$  in  $\widetilde{\mathbf{SL}_2\mathbf{R}}$  geometry. We develop a procedure to determine the densities of the above non-periodic optimal geodesic ball packings and apply this algorithm to them. We search for values of parameters  $p$  and  $q$  that provide the largest packing density. In this paper, we obtain greater density  $0.626606\dots$  for  $(p, q) = (29, 3)$  than the maximum density of the corresponding periodic geodesic ball packings under the groups  $\mathbf{pq2}_1$ .

In our work we use the projective model of  $\widetilde{\mathbf{SL}_2\mathbf{R}}$  introduced by Molnár in [2].

**1. Basic notions.** The real  $2 \times 2$  matrices  $\begin{pmatrix} d & b \\ c & a \end{pmatrix}$  with unit determinant  $ad - bc = 1$  constitute a Lie transformation group by the usual product operation, taken to act on row matrices as on point coordinates

---

2010 AMS *Mathematics subject classification.* Primary 51M20, 52B15, 52C17, 52C22, 53A35.

*Keywords and phrases.* Finite fields, permutation polynomials, Hermite-Dickson's theorem.

Received by the editors on March 13, 2014, and in revised form on August 9, 2014.

on the right as follows:

$$(1.1) \quad (z^0, z^1) \begin{pmatrix} d & b \\ c & a \end{pmatrix} = (z^0d + z^1c, z^0b + z^1a) = (w^0, w^1)$$

$$\text{with } w = \frac{w^1}{w^0} = \frac{b + (z^1/z^0)a}{d + (z^1/z^0)c} = \frac{b + za}{d + zc},$$

as action on the complex projective line  $\mathbf{C}^\infty$  (see [2, 3]). This group is a three-dimensional manifold, because of its three independent real coordinates and with its usual neighborhood topology ([8, 9, 16]). In order to model the above structure in the projective sphere  $\mathcal{PS}^3$  and in the projective space  $\mathcal{P}^3$  (see [2]), we introduce the new projective coordinates  $(x^0, x^1, x^2, x^3)$  where

$$a := x^0 + x^3, \quad b := x^1 + x^2, \quad c := -x^1 + x^2, \quad d := x^0 - x^3,$$

with the positive, then the non-zero multiplicative equivalence as projective freedom in  $\mathcal{PS}^3$  and in  $\mathcal{P}^3$ , respectively. Then it follows that  $0 > bc - ad = -x^0x^0 - x^1x^1 + x^2x^2 + x^3x^3$  describes the interior of the above one-sheeted hyperboloid solid  $\mathcal{H}$  in the usual Euclidean coordinate simplex with the origin  $E_0(1; 0; 0; 0)$  and the ideal points of the axes

$$E_1^\infty(0; 1; 0; 0), \quad E_2^\infty(0; 0; 1; 0), \quad E_3^\infty(0; 0; 0; 1).$$

We consider the collineation group  $\mathbf{G}_*$  that acts on the projective sphere  $\mathcal{SP}^3$  and preserves a polarity, i.e., a scalar product of signature  $(- - ++)$ , this group leaves the one sheeted hyperboloid solid  $\mathcal{H}$  invariant. We have to choose an appropriate subgroup  $\mathbf{G}$  of  $\mathbf{G}_*$  as an isometry group. Then the universal covering group and space  $\widetilde{\mathcal{H}}$  of  $\mathcal{H}$  will be the hyperboloid model of  $\widetilde{\mathbf{SL}}_2\mathbf{R}$ , [2].

The specific isometries  $\mathbf{S}(\phi)$ ,  $\phi \in \mathbf{R}$ , constitute a one parameter group given by the matrices:

$$(1.2) \quad \mathbf{S}(\phi) : (s_i^j(\phi)) = \begin{pmatrix} \cos \phi & \sin \phi & 0 & 0 \\ -\sin \phi & \cos \phi & 0 & 0 \\ 0 & 0 & \cos \phi & -\sin \phi \\ 0 & 0 & \sin \phi & \cos \phi \end{pmatrix}.$$

The elements of  $\mathbf{S}(\phi)$  are the so-called *fibre translations*. We obtain a unique fibre line to each  $X(x^0; x^1; x^2; x^3) \in \widetilde{\mathcal{H}}$  as the orbit under the right action of  $\mathbf{S}(\phi)$  on  $X$ . The coordinates of points lying on the fibre

line through  $X$  can be expressed as the images of  $X$  by  $\mathbf{S}(\phi)$ :

$$(1.3) \quad (x^0; x^1; x^2; x^3) \xrightarrow{\mathbf{S}(\phi)} (x^0 \cos \phi - x^1 \sin \phi; x^0 \sin \phi + x^1 \cos \phi; \\ x^2 \cos \phi + x^3 \sin \phi; -x^2 \sin \phi + x^3 \cos \phi).$$

The points of a fibre line through  $X$  by usual inhomogeneous Euclidean coordinates

$$x = \frac{x^1}{x^0}, \quad y = \frac{x^2}{x^0}, \quad z = \frac{x^3}{x^0}, \quad x^0 \neq 0$$

are given by

$$(1.4) \quad (1; x; y; z) \xrightarrow{\mathbf{S}(\phi)} \left( 1; \frac{x + \tan \phi}{1 - x \tan \phi}; \frac{y + z \tan \phi}{1 - x \tan \phi}; \frac{z - y \tan \phi}{1 - x \tan \phi} \right)$$

for the projective space  $\mathcal{P}^3$ , where ideal points (at infinity) conventionally occur.

In (1.3) and (1.4) we can see the  $2\pi$  periodicity of  $\phi$ , moreover the (logical) extension to  $\phi \in \mathbf{R}$ , as a real parameter, to have the universal covers  $\widetilde{\mathcal{H}}$  and  $\widetilde{\mathbf{SL}_2\mathbf{R}}$ , respectively, through the projective sphere  $\mathcal{PS}^3$ . The elements of the isometry group of  $\mathbf{SL}_2\mathbf{R}$  (and so by the above extension the isometries of  $\widetilde{\mathbf{SL}_2\mathbf{R}}$ ) can be described by the matrix  $(a_i^j)$ , see [2, 3]. Moreover, we have the projective proportionality, of course. We define the *translation group*  $\mathbf{G}_T$  as a subgroup of the isometry group of  $\mathbf{SL}_2\mathbf{R}$ , the isometries acting transitively on the points of  $\mathcal{H}$  and by the above extension on the points of  $\widetilde{\mathbf{SL}_2\mathbf{R}}$  and  $\widetilde{\mathcal{H}}$ .  $\mathbf{G}_T$  maps the origin  $E_0(1; 0; 0; 0)$  onto  $X(x^0; x^1; x^2; x^3)$ . These isometries and their inverses (up to a positive determinant factor) are given by the following matrices:

$$(1.5) \quad \mathbf{T} : (t_i^j) = \begin{pmatrix} x^0 & x^1 & x^2 & x^3 \\ -x^1 & x^0 & x^3 & -x^2 \\ x^2 & x^3 & x^0 & x^1 \\ x^3 & -x^2 & -x^1 & x^0 \end{pmatrix}.$$

The rotation about the fibre line through the origin  $E_0(1; 0; 0; 0)$  by angle  $\omega$  ( $-\pi < \omega \leq \pi$ ) can be expressed by the following matrix,

see [2],

$$(1.6) \quad \mathbf{R}_{E_0}(\omega) : (r_i^j(E_0, \omega)) = \begin{pmatrix} 1 & 0 & 0 & 0 \\ 0 & 1 & 0 & 0 \\ 0 & 0 & \cos \omega & \sin \omega \\ 0 & 0 & -\sin \omega & \cos \omega \end{pmatrix},$$

and the rotation  $\mathbf{R}_X(\omega)$  about the fibre line through  $X(x^0; x^1; x^2; x^3)$  by angle  $\omega$  can be derived by formulas (1.5) and (1.6):

$$(1.7) \quad \mathbf{R}_X(\omega) = \mathbf{T}^{-1} \mathbf{R}_{E_0}(\omega) \mathbf{T} : (r_i^j(X, \omega)).$$

Horizontal intersection of the hyperboloid solid  $\mathcal{H}$  with the plane  $E_0 E_2^\infty E_3^\infty$  provides the *hyperbolic  $\mathbf{H}^2$  base plane* of the model  $\tilde{\mathcal{H}} = \mathbf{SL}_2 \mathbf{R}$ . The fibre through  $X$  intersects the base plane  $z^1 = x = 0$  in the foot point

$$(1.8) \quad Z(z^0 = x^0 x^0 + x^1 x^1; z^1 = 0; z^2 = x^0 x^2 - x^1 x^3; z^3 = x^0 x^3 + x^1 x^2).$$

After [2], we introduce the so-called *hyperboloid parametrization* as follows:

$$(1.9) \quad \begin{aligned} x^0 &= \cosh r \cos \phi, & x^1 &= \cosh r \sin \phi, \\ x^2 &= \sinh r \cos(\theta - \phi), & x^3 &= \sinh r \sin(\theta - \phi), \end{aligned}$$

where  $(r, \theta)$  are polar coordinates of the base plane and  $\phi$  is just the fibre coordinate. We note that

$$-x^0 x^0 - x^1 x^1 + x^2 x^2 + x^3 x^3 = -\cosh^2 r + \sinh^2 r = -1 < 0.$$

The inhomogeneous coordinates corresponding to (1.9), that play an important role in the later visualization of prism tilings in  $\mathbf{E}^3$ , are given by

$$(1.10) \quad \begin{aligned} x &= \frac{x^1}{x^0} = \tan \phi, & y &= \frac{x^2}{x^0} = \tanh r \frac{\cos(\theta - \phi)}{\cos \phi}, \\ z &= \frac{x^3}{x^0} = \tanh r \frac{\sin(\theta - \phi)}{\cos \phi}. \end{aligned}$$

**1.1. Geodesic balls in  $\widetilde{\mathbf{SL}}_2\mathbf{R}$ .**

**Definition 1.1.** The *distance*  $d(P_1, P_2)$  between the points  $P_1$  and  $P_2$  is defined by the arc length of the geodesic curve from  $P_1$  to  $P_2$ .

**Definition 1.2.** The *geodesic sphere* of radius  $\rho$  (denoted by  $S_{P_1}(\rho)$ ) with the center at  $P_1$  is defined as the set of all points  $P_2$  satisfying  $d(P_1, P_2) = \rho$ . Moreover, we require that the geodesic sphere is a simply connected surface without self-intersection.

**Definition 1.3.** The body of the geodesic sphere of center  $P_1$  and with radius  $\rho$  is called *geodesic ball*, denoted by  $B_{P_1}(\rho)$ , i.e.,  $Q \in B_{P_1}(\rho)$  if and only if  $0 \leq d(P_1, Q) \leq \rho$ .

From the results [5] it follows that if  $\rho \in [0, \frac{\pi}{2})$  then  $S(\rho)$  is a simply connected surface in  $\mathbf{E}^3$  and  $\widetilde{\mathbf{SL}}_2\mathbf{R}$ , respectively. If  $\rho \geq \frac{\pi}{2}$  then the universal cover should be discussed. *Therefore, we consider geodesic spheres and balls only with radii  $\rho \in [0, \frac{\pi}{2})$  in what follows.*

**1.2. The volume of a geodesic ball.** The volume formula of the geodesic ball  $B(\rho)$  follows from the metric tensor  $g_{ij}$ , see [5]. We obtain the connection between the hyperboloid coordinates  $(r, \theta, \phi)$  and the geographical coordinates  $(s, \lambda, \alpha)$  in a standard way. Therefore, the volume of the geodesic ball of radius  $\rho$  can be computed by the following:

**Theorem 1.4.**

$$\begin{aligned}
 \text{Vol}(B(\rho)) &= \int_B \frac{1}{2} \sinh(2r) \, dr \, d\theta \, d\phi \\
 (1.11) \qquad &= 4\pi \int_0^\rho \int_0^{\pi/4} \frac{1}{2} \sinh(2r(s, \alpha)) |J_1| \, d\alpha \, ds \\
 &\quad + 4\pi \int_0^\rho \int_{\pi/4}^{\pi/2} \frac{1}{2} \sinh(2r(s, \alpha)) |J_2| \, d\alpha \, ds,
 \end{aligned}$$

where  $|J_1| = \left| \frac{\partial r/\partial s}{\partial \phi/\partial s} \frac{\partial r/\partial \alpha}{\partial \phi/\partial \alpha} \right|$  and similarly  $|J_2|$  (by Table 1 and  $\partial\theta/\partial\lambda = 1$ ) are the corresponding Jacobians.

**1.3. Regular bounded periodic prism tilings and their space groups  $\mathbf{pq2}_1$ .** In [14], we defined and described the regular prisms and prism tilings with a space group class  $\Gamma = \mathbf{pq2}_1$  of  $\widetilde{\mathbf{SL}}_2\mathbf{R}$ . These will be summarized in this section.

**Definition 1.5.** Let  $\mathcal{P}^i$  be an infinite solid that is bounded by certain surfaces determined (as in [14]) by “side fibre lines” passing through the vertices of a regular  $p$ -gon  $\mathcal{P}^b$  lying in the base plane. The images of solids  $\mathcal{P}^i$  by  $\widetilde{\mathbf{SL}}_2\mathbf{R}$  isometries are called *infinite regular  $p$ -sided prisms*. Here, *regular* means that the side surfaces are congruent to each other under rotations about a fiber line (e.g., through the origin).

The common part of  $\mathcal{P}^i$ , with the base plane is the *base figure* of  $\mathcal{P}^i$  that is denoted by  $\mathcal{P}$  and its vertices coincide with the vertices of  $\mathcal{P}^b$ , but  $\mathcal{P}$  is not assumed to be a polygon.

**Definition 1.6.** A *bounded regular  $p$ -sided prism* is an isometric image of a solid which is bounded by the side surfaces of a regular  $p$ -sided infinite prism  $\mathcal{P}^i$ , its base figure  $\mathcal{P}$  and the translated copy  $\mathcal{P}^t$  of  $\mathcal{P}$  by a fibre translation, given by (1.2). The faces  $\mathcal{P}$  and  $\mathcal{P}^t$  are called *cover faces*.

We consider regular prism tilings  $\mathcal{T}_p(q)$  by prisms  $\mathcal{P}_p(q)$  where  $q$  pieces regularly meet at each side edge by  $q$ -rotation.

The following theorem has been proved in [14].

**Theorem 1.7.** *There exist regular, bounded prism tilings  $\mathcal{T}_p(q)$  in  $\widetilde{\mathbf{SL}}_2\mathbf{R}$  that are not face-to-face for all integers  $p$  and  $q$  such that  $3 \leq p$  and  $2p/(p-2) < q$ .*

We assume that the prism  $\mathcal{P}_p(q)$  is a *topological polyhedron* having at each vertex one  $p$ -gonal cover face (it is not a polygon at all) and two *skew quadrangles* which lie on certain side surfaces in the model. Let  $\mathcal{P}_p(q)$  be one of the tiles of  $\mathcal{T}_p(q)$ ;  $\mathcal{P}^b$  is centered in the origin with vertices  $A_1A_2A_3 \cdots A_p$  in the base plane (Figures 1 and 2). It is clear that the side curves,  $c_{A_iA_{i+1}}$ ,  $i = 1, \dots, p$ ,  $A_{p+1} \equiv A_1$ , of the base figure are derived from each other by  $2\pi/p$  rotation about the vertical

$x$  axis, so they are congruent in the  $\widetilde{\mathbf{SL}}_2\mathbf{R}$  sense. The corresponding vertices  $B_1B_2B_3 \cdots B_p$  are generated by a fibre translation  $\tau$  given by (1.3) with real parameter  $\Phi > 0$ . The fibre lines through the vertices  $A_iB_i$  are denoted by  $f_i$ ,  $i = 1, \dots, p$ , and the fibre line through the “midpoint”  $H$  of the curve  $c_{A_1A_p}$  is denoted by  $f_0$ . This  $f_0$  will be a half-screw axis as follows below.

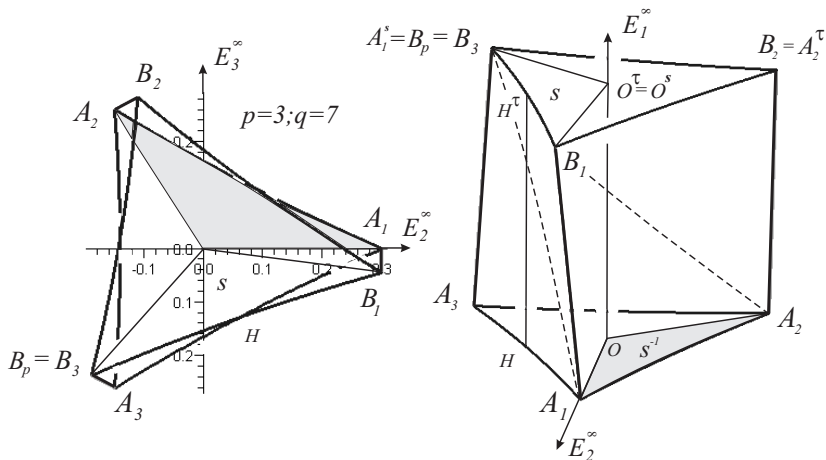


FIGURE 1. The regular prism  $\mathcal{P}_p(q)$  and the fundamental domain of the space group  $\mathbf{pq2}_1$

The tiling  $\mathcal{T}_p(q)$  is generated by a discrete isometry group  $\Gamma_p(q) = \mathbf{pq2}_1 \subset \text{Isom}(\widetilde{\mathbf{SL}}_2\mathbf{R})$  given by its fundamental domain  $A_1A_2OA_1^sA_2^sO^s$  a *topological polyhedron* and the group presentation (see Figures 1 and 4 for  $p = 3$  and [14] for details):

$$(1.12) \quad \begin{aligned} \mathbf{pq2}_1 &= \{ \mathbf{a}, \mathbf{b}, \mathbf{s} : \mathbf{a}^p = \mathbf{b}^q = \mathbf{asa}^{-1}\mathbf{s}^{-1} = \mathbf{babs}^{-1} = \mathbf{1} \} \\ &= \{ \mathbf{a}, \mathbf{b} : \mathbf{a}^p = \mathbf{b}^q = \mathbf{ababa}^{-1}\mathbf{b}^{-1}\mathbf{a}^{-1}\mathbf{b}^{-1} = \mathbf{1} \}. \end{aligned}$$

Here  $\mathbf{a}$  is a  $p$ -rotation about the fibre line through the origin ( $x$  axis),  $\mathbf{b}$  is a  $q$ -rotation about the fibre line trough  $A_1$  and  $\mathbf{s} = \mathbf{bab}$  is a screw motion  $\mathbf{s} : OA_1A_2 \rightarrow O^sB_pB_1$ . All these can be obtained by formulas (1.5) and (1.6). Then we get that  $\mathbf{abab} = \mathbf{baba} =: \tau$  is a fibre translation. Then  $\mathbf{ab}$  is a  $\mathbf{2}_1$  half-screw motion about  $f_0 = HH^\tau$  (see Figure 1) that also determines the fibre translation  $\tau$  above. This

group in (3.1) surprisingly occurred in [6, Section 6] at double links  $K_{p,q}$ . The coordinates of the vertices  $A_1A_2A_3 \cdots A_p$  of the base figure and the corresponding vertices  $B_1B_2B_3 \cdots B_p$  of the cover face can be computed for all given parameters  $p, q$  by

$$(1.13) \quad \tanh(OA_1) = b := \sqrt{\frac{1 - \tan \pi/p \tan \pi/q}{1 + \tan \pi/p \tan \pi/q}}.$$

**1.4. The volume of the bounded regular prisms.** The volume formula of a *sector-like* three dimensional domain  $\text{Vol}(D(\Psi))$  can be computed routinely by the metric tensor  $g_{ij}$ , see [5], in the hyperboloid coordinates. This is defined by the base figure  $D$  lying in the base plane and by fibre translation  $\tau$  given by (1.3) with the height parameter  $\Psi$ .

**Theorem 1.8.** *Suppose we are given a sector-like region  $D$ , a continuous function  $r = r(\theta)$ , where the radius  $r$  depends upon the polar angle  $\theta$ . The volume of the domain  $D(\Psi)$  is derived by the following integral:*

$$(1.14) \quad \begin{aligned} \text{Vol}(D(\Psi)) &= \int_D \frac{1}{2} \sinh(2r(\theta)) / r, dr d\theta d\psi \\ &= \int_0^\Psi \int_{\theta_1}^{\theta_2} \int_0^{r(\theta)} \frac{1}{2} \sinh(2r(\theta)) dr d\theta d\psi \\ &= \Psi \int_{\theta_1}^{\theta_2} \frac{1}{4} (\cosh(2r(\theta)) - 1) d\theta. \end{aligned}$$

Letting  $\mathcal{P}_p(q)$  be an arbitrary bounded regular prism, we get the following.

**Theorem 1.9.** *The volume of the bounded regular prism  $\mathcal{P}_p(q)$  ( $3 \leq p \in \mathbb{N}$ ,  $2p/(p-2) < q \in \mathbb{N}$ ) is given by the following simple formula:*

$$(1.15) \quad \text{Vol}(\mathcal{P}_p(q)) = \text{Vol}(D(p, q, \Psi)) \cdot p,$$

where  $\text{Vol}(D(p, q, \Psi))$  is the volume of the sector-like three dimensional domain given by the sector region  $OA_1A_2 \subset \mathcal{P}$  (see Figures 1 and 3) and by  $\Psi$ , the  $\widetilde{\text{SL}}_2\mathbb{R}$  height of the prism, depending on  $p, q$ .

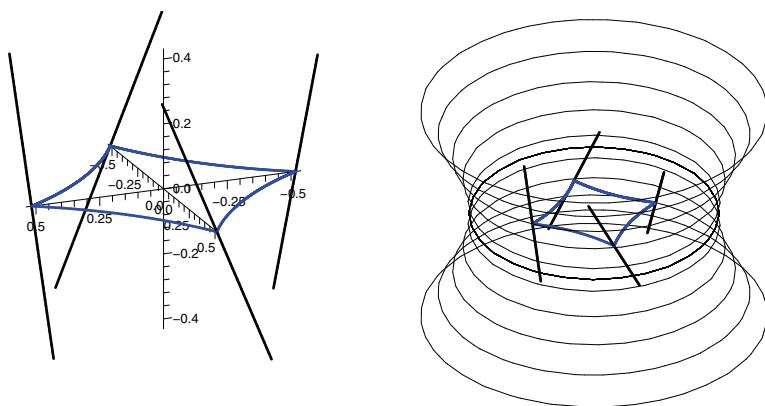


FIGURE 2. Regular infinite 4-gonal prism  $\mathcal{P}_4^i(6)$  of the infinite regular prism tiling  $\mathcal{T}_4^i(6)$ .

## 2. Regular infinite prism tilings and non-periodic ball packings.

**2.1. Infinite regular prism tilings.** In this subsection, we study the regular infinite prism tilings  $\mathcal{T}_p^i(q)$ . Let  $\mathcal{T}_p(q)$  be a regular prism tiling, and let  $\mathcal{P}_p(q)$  be one of its tiles given by its base figure  $\mathcal{P}$ , centered at the origin  $K$  with vertices  $G_1G_2G_3 \cdots G_p$  in the base plane of the model and the corresponding vertices  $A_1A_2A_3 \cdots A_p$  and  $B_1B_2B_3 \cdots B_p$  generated by fibre translations  $-\tau$  and  $\tau$  given by (1.3) with parameter  $\Psi = \pi/2 - \pi/p - \pi/q$ . The images of the topological polyhedron  $\mathcal{P}_p(q)$  by the translations  $\langle \tau \rangle$  form an infinite prism  $\mathcal{P}_p^i(q)$  (see Definitions 1.5 and 1.6).

By the construction of the bounded prism tilings it follows that the rotation through  $\omega = 2\pi/q$  about the fibre lines  $f_i$  maps the corresponding side face onto the neighboring one. Therefore, we obtain the following (see [14]):

**Theorem 2.1.** *There exist regular infinite face-to-face prism tilings  $\mathcal{T}_p^i(q)$  for integer parameters  $p \geq 3$  and  $q > 2p/(p - 2)$ .*

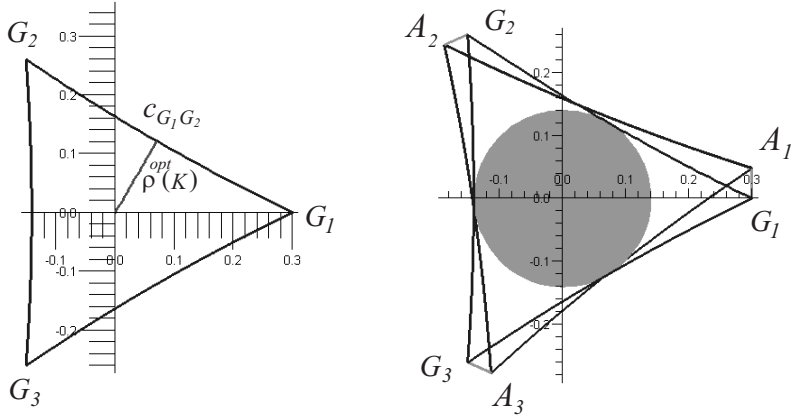


FIGURE 3. The maximum radius  $\rho^{opt}(K)$  and the optimal half-prism  $A_1A_2A_3G_1G_2G_3$  with the optimal half-sphere for parameters  $p = 3, q = 7$  with the maximum radius

For example, we have described  $\mathcal{P}_4^i(6)$  with its base polygon in Figure 2, with  $b = (\sqrt{6} - \sqrt{2})/2$ .

**2.2. Non-periodic geodesic ball packings.** We consider an infinite regular prism tiling  $\mathcal{T}_p^i(q)$  and let  $\mathcal{P}_p^i(q)$  be one of its tiles with base figure  $\mathcal{P}$  centered at the origin with vertices  $G_1G_2 \cdots G_p$  in the base plane of the model. Let  $B_K^{opt}$  be the geodesic ball with center at the origin  $K$  that touches the side surfaces of the infinite regular prism  $\mathcal{P}_p^i(q)$ . The radius of the ball  $B_K^{opt}$  is denoted by  $\rho^{opt}(K)$ . Moreover, we define the regular prism  $\mathcal{P}_p^{opt}(q) = A_1A_2 \cdots A_pB_1B_2 \cdots B_p$  with base figure  $\mathcal{P}$  and with cover faces  $A_1A_2 \cdots A_p$  and  $B_1B_2 \cdots B_p$  touching  $B_K^{opt}$ . It is clear that the height  $h_p^{opt}(q)$  of  $\mathcal{P}_p^{opt}(q)$  is  $2\rho^{opt}(K)$ .

The images of  $\mathcal{P}_p^{opt}(q)$  by the fibre translations  $\langle \tau \rangle$  where  $h_p^{opt}(q) = |\tau| = 2\rho^{opt}(K)$  covers the infinite regular prism  $\mathcal{P}_p^i(q)$  and by the structure of the infinite prism tilings follows the rotations through  $\omega = 2\pi/q$  about the fibre lines.  $f_i$  maps the corresponding side face onto the neighboring one and thus the images of  $\mathcal{P}_p^{opt}(q)$  fill the  $\widetilde{\mathbf{SL}_2\mathbf{R}}$  space without overlap. These tilings are denoted by  $\mathcal{T}_p^n(q)$ .

The height  $h_p^{\text{opt}}(q)$  of the prism  $\mathcal{P}_p^{\text{opt}}(q)$  is not equal to  $\pi - 2\pi/p - 2\pi/q$  so the corresponding regular prism tiling is non-periodic. We note here that there are infinitely many non-periodic prism tilings derived from  $\mathcal{T}_p^n(q)$ .

For the density of the packing it is sufficient to relate the volume of the optimal ball to that of the solid  $\mathcal{P}_p^{\text{opt}}(q)$ . The density of the optimal ball packing of the prism tiling  $\mathcal{T}_p^n(q)$  (with integer parameters  $p \geq 3$  and  $q > 2p/(p - 2)$ ) can be computed by the formula:

$$\delta_p^{\text{opt}}(q) := \frac{\text{Vol}(B_K^{\text{opt}})}{\text{Vol}(\mathcal{P}_p^{\text{opt}}(q))}.$$

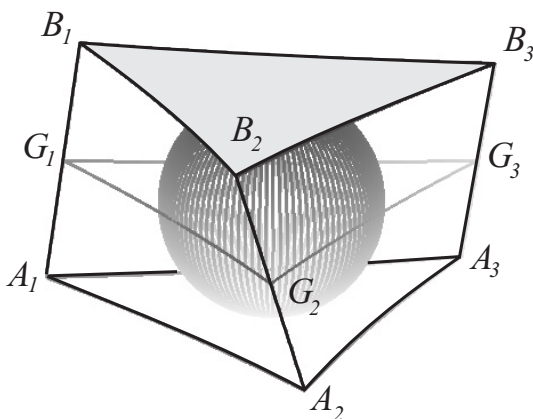


FIGURE 4. The optimal prism  $A_1A_2A_3B_1B_2B_3$  with optimal sphere for parameters  $p = 3, q = 7$ , of maximum radius  $\rho^{\text{opt}}(K)$

In order to determine the optimal radius  $\rho^{\text{opt}}(K)$  we will use the following lemmas.

**Lemma 2.2.** *The parametric equation of the side curve  $c_{G_1G_2}$  of the base figure  $\mathcal{P}$  is*

$$c_p^q(t) = \left( 0, \sqrt{\sin\left(\frac{2\pi}{p} + \frac{2\pi}{q}\right)} \left( t \cos\left(\frac{2\pi}{p}\right) \sin^2\left(\frac{\pi}{p} + \frac{\pi}{q}\right) \right) \right)$$

$$\begin{aligned}
& -\frac{t}{2} \sin\left(\frac{2\pi}{p}\right) \sin\left(\frac{2\pi}{p} + \frac{2\pi}{q}\right) + \sin^2\left(\frac{\pi}{p} + \frac{\pi}{q}\right)(1-t) \\
& + t^2 \cos\left(\frac{\pi}{p} + \frac{\pi}{q}\right) \cos\left(\frac{\pi}{p} - \frac{\pi}{q}\right) \Big/ \\
(2.1) \quad & \cdot \left( \sqrt{\left(\sin\left(\frac{2\pi}{p}\right) + \sin\left(\frac{2\pi}{q}\right)\right)} \right. \\
& \cdot \left. \left( \sin^2\left(\frac{\pi}{p} + \frac{\pi}{q}\right) + t^2 \cos^2\left(\frac{\pi}{p} + \frac{\pi}{q}\right) \right) \right), \\
& \sqrt[t]{\sin\left(\frac{2\pi}{p} + \frac{2\pi}{q}\right) \left( \sin\left(\frac{2\pi}{p}\right) \sin^2\left(\frac{\pi}{p} + \frac{\pi}{q}\right) \right.} \\
& + \frac{1}{2} \cos\left(\frac{2\pi}{p}\right) \sin\left(\frac{2\pi}{p} + \frac{2\pi}{q}\right)(1-t) \\
& + \cos\left(\frac{\pi}{p} + \frac{\pi}{q}\right) \left( t \sin\left(\frac{2\pi}{p}\right) \cos\left(\frac{\pi}{p} + \frac{\pi}{q}\right) \right. \\
& \left. \left. + \sin\left(\frac{\pi}{p} + \frac{\pi}{q}\right)(t-1) \right) \right) \Big/ \\
& \cdot \left( \sqrt{\left(\sin\left(\frac{2\pi}{p}\right) + \sin\left(\frac{2\pi}{q}\right)\right)} \right. \\
& \cdot \left. \left( \sin^2\left(\frac{\pi}{p} + \frac{\pi}{q}\right) + t^2 \cos^2\left(\frac{\pi}{p} + \frac{\pi}{q}\right) \right) \right), \quad t \in [0, 1].
\end{aligned}$$

The equation of the side curve  $c_{G_1 G_2}$  is derived by formulas (1.3) and (1.8). Therefore, they are congruent and their curvatures are equal in the  $\widetilde{\mathbf{SL}_2\mathbf{R}}$  sense. Moreover, the side curves are also congruent in the Euclidean sense; therefore, their curvatures are equal in the Euclidean sense as well. Our next lemma is obtained by applying some routine techniques commonly used in differential geometry.

**Lemma 2.3.** *The curvature  $C_p(q)$  of the side curves  $c_{G_i G_{i+1}}$ ,  $i = 1, \dots, p$ ,  $G_{p+1} \equiv G_1$ , in the Euclidean sense is*

$$(2.2) \quad C_p(q) = \sqrt{\frac{\cos(\pi/p + \pi/q) (\sin(2\pi/p) + \sin(2\pi/q))}{\sin(\pi/p + \pi/q) (1 - \cos(2\pi/p))}};$$

therefore, the side curves  $c_{G_i G_{i+1}}$  ( $i = 1, \dots, p$ ,  $G_{p+1} \equiv G_1$ ) are Euclidean circular arcs of radius  $r_p^q = 1/C_p(q)$ .

**Remark 2.4.**

(i) It is easy to see that the asymptotic behavior of  $C_p(q)$  is as follows:

$$\lim_{q \rightarrow \infty} (C_p(q)) = \cot\left(\frac{\pi}{p}\right), \quad \lim_{p \rightarrow \infty} (C_p(q)) = \infty.$$

(ii) Given a line and a point not on it, let  $x$  be the distance from the point to the line along the perpendicular segment dropped from the point to the line. Let  $\phi = \Pi(x)$  be the least angle, such that the line drawn through the point at that angle does not intersect the given line. This angle is called the *angle of parallelism*. By the famous formula of J. Bolyai it follows that  $\log(\cot(\phi)) = x$ . Therefore, if we denote the distance of parallelism of the angle  $\phi$  by  $\Lambda(\phi)$ , then

$$\log\left(\lim_{q \rightarrow \infty} (C_p(q))\right) = \log\left(\cot\left(\frac{\pi}{p}\right)\right) = \Lambda\left(\frac{\pi}{p}\right).$$

Table 1 lists the radii of curvature  $r_3^q$  of the side curve  $c_{G_1 G_2}$  of the base figure  $\mathcal{P}$ .

| Table 1  |          |          |          |           |
|----------|----------|----------|----------|-----------|
| $(p, q)$ | (3, 7)   | (3, 8)   | (3, 10)  | (3, 1000) |
| $C_p(q)$ | 0.286926 | 0.371579 | 0.453885 | 0.577339  |
| $r_p^q$  | 3.485219 | 2.691215 | 2.203203 | 1.732085  |

The maximum radius  $\rho^{\text{opt}}(K)$  of the balls  $B_K^{\text{opt}}$  can be determined by applying the above lemmas for all possible parameters as the distance between the origin and  $c_{G_1 G_2}$ . The volumes  $\text{Vol}(B_K^{\text{opt}})$  can be computed by Theorem 1.8, and the volumes of the prisms  $\mathcal{P}_p^{\text{opt}}(q)$  can be determined by Theorem 1.9.

The above locally dense geodesic ball packings can be determined for all regular prism tilings  $\mathcal{T}_p^n(q)$  ( $p, q$  as above); our results are summarized in Tables 2 and 3.

**Remark 2.5.**

- (i) The best density that we found is approximately 0.626606, attained at parameters  $p = 29, q = 3$ , that is greater than the maximum density of the corresponding periodic geodesic ball packings under the groups  $\mathbf{pq2}_1$ .
- (ii) The problems of finding the densest geodesic and translation ball packings are timely and intensively investigated in other Thurston geometries, as well (see e.g., [4, 10, 11, 12, 13]).

Table 2.

| $(p, q)$ | $\rho^{\text{opt}}(K)$ | $\text{Vol}(B_K^{\text{opt}})$ | $\text{Vol}(\mathcal{P}_p^{\text{opt}}(q))$ | $\delta_p^{\text{opt}}(q)$ |
|----------|------------------------|--------------------------------|---|----------------------------|
| (3,7)    | 0.141564               | 0.011963                       | 0.031767                                    | 0.376592                   |
| (3,8)    | 0.181760               | 0.025431                       | 0.071377                                    | 0.356287                   |
| (3,10)   | 0.219795               | 0.045198                       | 0.138101                                    | 0.327281                   |
| (3,1000) | 0.274648               | 0.088981                       | 0.428828                                    | 0.207499                   |
| $\vdots$ | $\vdots$               | $\vdots$                       | $\vdots$                                    | $\vdots$                   |
| (4,5)    | 0.265319               | 0.080085                       | 0.166705                                    | 0.480397                   |
| (4,6)    | 0.329239               | 0.154965                       | 0.344779                                    | 0.449464                   |
| (4,10)   | 0.404230               | 0.292043                       | 0.761956                                    | 0.383280                   |
| (4,1000) | 0.440683               | 0.382228                       | 1.378910                                    | 0.277196                   |
| $\vdots$ | $\vdots$               | $\vdots$                       | $\vdots$                                    | $\vdots$                   |
| (5,4)    | 0.313435               | 0.133256                       | 0.246171                                    | 0.541312                   |
| (5,5)    | 0.421241               | 0.332010                       | 0.661684                                    | 0.501765                   |
| (5,10)   | 0.530638               | 0.686600                       | 1.667047                                    | 0.411866                   |
| (5,1000) | 0.562086               | 0.825191                       | 2.639937                                    | 0.312580                   |
| $\vdots$ | $\vdots$               | $\vdots$                       | $\vdots$                                    | $\vdots$                   |
| (6,4)    | 0.440687               | 0.382237                       | 0.692229                                    | 0.552183                   |
| (6,5)    | 0.530638               | 0.686600                       | 1.333638                                    | 0.514833                   |
| (6,10)   | 0.629251               | 1.188024                       | 2.767592                                    | 0.429263                   |
| (6,1000) | 0.658476               | 1.377893                       | 4.124915                                    | 0.334042                   |
| $\vdots$ | $\vdots$               | $\vdots$                       | $\vdots$                                    | $\vdots$                   |
| (7,3)    | 0.272637               | 0.087010                       | 0.142753                                    | 0.609513                   |
| (7,4)    | 0.535202               | 0.705586                       | 1.261041                                    | 0.559527                   |
| (7,5)    | 0.617496               | 1.117400                       | 2.133913                                    | 0.523639                   |
| (7,10)   | 0.710652               | 1.772033                       | 4.018646                                    | 0.440953                   |

Table 2 (Continued).

| $(p, q)$ | $\rho^{\text{opt}}(K)$ | $\text{Vol}(B_K^{\text{opt}})$ | $\text{Vol}(\mathcal{P}_p^{\text{opt}}(q))$ | $\delta_p^{\text{opt}}(q)$ |
|----------|------------------------|--------------------------------|---|----------------------------|
| (7,1000) | 0.738668               | 2.015812                       | 5.785244                                    | 0.348440                   |
| $\vdots$ | $\vdots$               | $\vdots$                       | $\vdots$                                    | $\vdots$                   |
| (8,3)    | 0.382143               | 0.245334                       | 0.400179                                    | 0.613062                   |
| (8,4)    | 0.612113               | 1.086117                       | 1.923010                                    | 0.564800                   |
| (8,5)    | 0.690221               | 1.608804                       | 3.035751                                    | 0.529953                   |
| (8,10)   | 0.780165               | 2.422804                       | 5.392115                                    | 0.449324                   |
| (8,1000) | 0.807443               | 2.722797                       | 7.589676                                    | 0.358750                   |
| $\vdots$ | $\vdots$               | $\vdots$                       | $\vdots$                                    | $\vdots$                   |

Table 3.

| $(p, q)$       | $\rho^{\text{opt}}(K)$ | $\text{Vol}(B_K^{\text{opt}})$ | $\text{Vol}(\mathcal{P}_p^{\text{opt}}(q))$ | $\delta_p^{\text{opt}}(q)$ |
|----------------|------------------------|--------------------------------|---|----------------------------|
| (10, 3)        | 0.530638               | 0.686600                       | 1.111365                                    | 0.617799                   |
| $\vdots$       | $\vdots$               | $\vdots$                       | $\vdots$                                    | $\vdots$                   |
| (20, 3)        | 0.914848               | 4.195479                       | 6.706186                                    | 0.625613                   |
| (20, 4)        | 1.094612               | 8.023914                       | 13.755306                                   | 0.583332                   |
| (20, 5)        | 1.163424               | 10.092704                      | 18.275027                                   | 0.552268                   |
| (20, 10)       | 1.245625               | 13.132701                      | 27.392724                                   | 0.479423                   |
| (20, 1000)     | 1.271043               | 14.216772                      | 35.858024                                   | 0.396474                   |
| $\vdots$       | $\vdots$               | $\vdots$                       | $\vdots$                                    | $\vdots$                   |
| (28, 3)        | 1.088398               | 7.855861                       | 12.537440                                   | 0.626592                   |
| <b>(29, 3)</b> | <b>1.106311</b>        | <b>8.348310</b>                | <b>13.323054</b>                            | <b>0.626606</b>            |
| (30, 3)        | 1.123593               | 8.847342                       | 14.119487                                   | 0.626605                   |
| $\vdots$       | $\vdots$               | $\vdots$                       | $\vdots$                                    | $\vdots$                   |
| (35, 3)        | 1.201914               | 11.432334                      | 18.250297                                   | 0.626419                   |
| $\vdots$       | $\vdots$               | $\vdots$                       | $\vdots$                                    | $\vdots$                   |
| (40, 3)        | 1.269482               | 14.148085                      | 22.599777                                   | 0.626028                   |
| $\vdots$       | $\vdots$               | $\vdots$                       | $\vdots$                                    | $\vdots$                   |
| (52, 3)        | 1.401728               | 21.089811                      | 33.761388                                   | 0.624673                   |
| $\vdots$       | $\vdots$               | $\vdots$                       | $\vdots$                                    | $\vdots$                   |
| (72, 3)        | 1.565173               | 33.642710                      | 54.088487                                   | 0.621994                   |

## REFERENCES

1. K. Böröczky and A. Florian, *Über die dichteste Kugelpackung im hyperbolischen Raum*, Acta Math. Hung. **15** (1964), 237–245.
2. E. Molnár, *The projective interpretation of the eight 3-dimensional homogeneous geometries*, Beitr. Alg. Geom. **38** (1997), 261–288.
3. E. Molnár and J. Szirmai, *Symmetries in the 8 homogeneous 3-geometries*, Symmetry Cult. Sci. **21** (2010), 87–117.
4. ———, *Classification of Sol lattices*, Geom. Ded. **161** (2012), 251–275.
5. ———, *Volumes and geodesic ball packings to the regular prism tilings in  $\widetilde{\mathbf{SL}}_2\mathbf{R}$  space*, Publ. Math. Debr. **84** (2014), 189–203.
6. E. Molnár, J. Szirmai and A. Vesnin, *Projective metric realizations of cone-manifolds with singularities along 2-bridge knots and links*, J. Geom. **95** (2009), 91–133.
7. ———, *Packings by translation balls in  $\widetilde{\mathbf{SL}}_2\mathbf{R}$* , J. Geom. **105** (2014), 287–306.
8. J.G. Ratcliffe, *Foundations of hyperbolic manifolds*, 2nd ed, Grad. Texts Math. **149**, Springer, New York, 2006.
9. P. Scott, *The geometries of 3-manifolds*, Bull. Lond. Math. Soc. **15** (1983), 401–487.
10. J. Szirmai, *The densest geodesic ball packing by a type of Nil lattices*, Beitr. Alg. Geom. **48** (2007), 383–398.
11. ———, *Geodesic ball packing in  $\mathbf{S}^2 \times \mathbf{R}$  space for generalized Coxeter space groups*, Beitr. Alg. Geom. **52** (2011), 413–430.
12. ———, *Geodesic ball packing in  $\mathbf{H}^2 \times \mathbf{R}$  space for generalized Coxeter space groups*, Math. Comm. **17** (2012), 151–170.
13. ———, *Lattice-like translation ball packings in Nil space*, Publ. Math. Debrecen **80** (2012), 427–440.
14. ———, *Regular prism tilings in  $\widetilde{\mathbf{SL}}_2\mathbf{R}$  space*, Aequat. Math. **88** (2014), 67–79.
15. ———, *A candidate to the densest packing with equal balls in the Thurston geometries*, Beitr. Alg. Geom. (2013).
16. W.P. Thurston and S. Levy, eds., *Three-dimensional geometry and topology*, Princeton University Press, Princeton, 1997.

BUDAPEST UNIVERSITY OF TECHNOLOGY AND ECONOMICS INSTITUTE OF MATHEMATICS, DEPARTMENT OF GEOMETRY, P.O. BOX 91, BUDAPEST H-1521, HUNGARY  
**Email address:** szirmai@math.bme.hu